Original paper

Study of Behavior of Concrete-confined Steel Composite Columns in Frame

Arash Bayat

Department of Civil Engineering, Razi University, Kermanshah, Iran.

ARTICLE INFO

ABSTRACT

In this research the behavior of frame with concrete-confined steel composite column is studied. In turn, three dimensional (3D) finite element nonlinear model is used for analysis of inelastic behavior of concrete, steel, longitudinal reinforcements, transverse reinforcements and also the effect of concrete confinement for concrete-confined steel composite columns and the modeling procedure is performed by ABAQUS software. Three types of frame composed of concrete-confined steel composite columns with SRC beam, steel section beam, and reinforced concrete beam are modeled and the effects of parameters of compressive strengths of concrete and yield tension of steel section on the frame behavior and strength are studied for each one of these three frames. The results show that increasing these two parameters improves and increases the behavior of frame and its strength. The effect of increasing compressive strengths of concrete for SRC beam frame and also the effect of increasing yield tension of steel section is more pronounced for steel section frame, while increasing both parameters for reinforced concrete beam frame has almost identical effect on increasing and improving the frame behavior.

1. Introduction

In recent years using composite columns is increased in advanced countries due to the numerous advantages comparing to normal reinforced concrete and steel columns. Some of these advantages are high ductility, good strength with lower volume and weight comparing to reinforced concrete columns, high strength against fire, being cost-effective and less deformation comparing to steel columns and no local buckling in concreted-covered steel columns comparing to normal steel columns.

Composite columns are divided into two broad groups in lights of concrete and steel embodiment:

A: Concrete-confined steel sections which are also called "steel reinforced concrete".

B: Concreted-filled tube.

Many studies are performed regarding the first type and it is used due to its simple implementation; but less studies are performed about the second type, for example:

Kong et al. (2013) studied the frame behavior under the cyclic and uniform load in a parametric modeling analysis and their results show that increasing steel ratio has a meaningful effect on the final capacity and seismic performance of the frame [1].

Kong et al. (2013) studied the effect of effective factors on behavior of SRC composite columns frame and their results show that the steel sections form ratio has a meaningful effect on improving final loading and seismic performance of structure frame, while axial force ratio has no meaningful effect [2].

Li et al. (2015) studied the mechanical behavior of concrete-confined steel composite columns in comparison with reinforced concrete columns under static and cyclic loading and their results show that loading and ductility capacity of SRC columns under static loading is magnificently higher than reinforced concrete columns and also under the cyclic loading, the hysteresis diagrams of SRC columns are fuller than reinforced concrete columns [3].

Besides reviewing the statute design of concrete-confined steel composite columns, Alavi and Izadinia (2012) in their research also explained the modeling of these columns by applying the effect of confinement in ABAQUS software [4].

Kheyroldin et al. (2012) studied the presented relationships for concrete confinement in cycle composite columns filled by concrete and their results show that many advantages of composite columns is dependent on the interaction between steel and concrete and there are many ambiguities regarding good interactions of concrete and steel [5].

This research is performed due to large number of steel buildings and the possibility reinforcing them with this method and also the higher strength against fire in comparison to concrete filled tubes.

Beiranvand et al. (2019) studied the investigation of load capacity of steel concrete composite columns SRC reinforced by IPE. Their results showed that the load capacity of the column, with increasing length and also increasing eccentricity of the axial load, will be reduced. With increasing

*Corresponding author Email: abayat@razi.ac.ir

length, the effect of an increased eccentricity of the reduced load capacity was increased [6].

Although steel-concrete composite columns have been used extensively for more than 50 years in buildings and other structures and this trend is increasing in worldwide, however these columns are still considered as reinforced concrete and steel columns in lights of design and the concrete and steel interaction is ignored. Effective and efficient usage of composite columns requires a different attitude for steel and concrete columns so this process can be started.

Recently modeling samples of concrete by different software are taken into consideration. One of the strong finite element software is ABAQUS which is used here. Many challenges in experimental works have led the researchers to pay their attention to modeling procedure in software. Experimental works require higher cost, time, labor, etc. Also experimental errors, limitations in loading, loading conditions, the number of constructed samples, and the inability to construct some samples are some challenges that exist in experimental words. The challenges in modeling are far less and better results are achieved from analysis. For example, any sample under any type of loading can be modeled in software and different parameters can be studied, while every experimental sample is used under one type and one loading value and only for achieving one parameter.

In this research the behavior of frame with concrete-confined steel composite column is studied. In turn, finite element nonlinear three dimensional (3D) model is used for analysis of inelastic behavior of concrete, steel, longitudinal reinforcements, transverse reinforcements and also the effect of concrete confinement for concrete-confined steel composite columns and the modeling procedure is performed by ABAQUS software.

2. Materials and Methods

Concrete-confined steel column under study in this research is composed of four components which are steel section, longitudinal reinforcements, transverse reinforcements, and concrete which are shown in Fig. 1. The previous literatures by Mirza [7] on reinforced concrete columns show that concrete columns are divided into two areas based on reinforcements. One area is internal effective concrete-confined core and the other area is external ineffective non-confined area which includes cover concrete and parabolic part of concrete between reinforcement bars (Fig. 1).

In steel composite columns with concrete cover, the concrete confinement is provided by steel section and reinforcement bars. Concrete confinement depends on many factors including steel section form, diameter, gridding, distance, and number of longitudinal reinforcements and also the diameter and distance of transverse reinforcements. In addition to these factors, yield tension of steel section and reinforcements such as concrete compressive strength affect the confinement. Increase of strength and concrete ductility are the results of the confinement pressure which its value. Due to this confinement, concrete in composite column is divided into three main area including:

A: Unconfined concrete which is created in area outside the parabolic arc by the reinforcements.

B: Area with high confinement which is created inside the steel section part of the structure and arc.

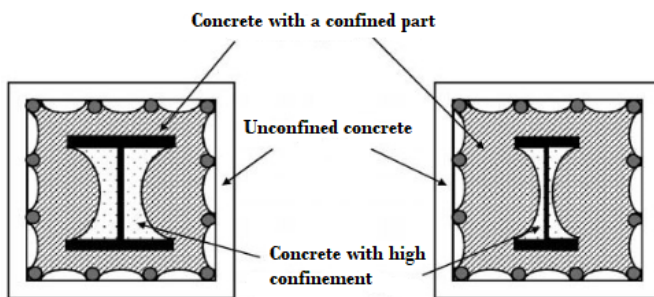Area with partial confinement which is between two areas with high confinement and without confinement (Fig. 1).

Fig 1. Confinement area in concrete-confined steel composite column.

In their analytic research which was performed by different forms of steel sections and different patterns of gridding reinforcement bar, Chen and Lin [8] studied the confinement factors for concrete area with high confinement and concrete with partial confinement and Mirza and Skrabek [9] in their research showed that these parabolic area can be simplified and be considered as rectangles. In this way, concrete with high confinement is placed along the steel section web to half width of steel section flange and concrete with partial confinement is placed from half width of steel section flanges along the section flange until the center line of longitudinal reinforcements and finally the unconfined concrete remains as the external area.

2.1. Concrete

Considering the necessity of 3D modeling and in order to assign an element with secures the concrete behavior in this state, we can use 3D, 8-node elements "C3D8R". R suffix is used in order to reduce the integrating points' number so the program implementation time would be reduced.

Reasons to select this type of element is less convergence problem and higher answer precision. One of the disadvantages of this element is very hard meshing of the models and also damage plasticity method in nonlinear are is used for concrete behavior fundamental equation.

The effect of concrete confinement is recognized by the lateral reinforcements in reinforced concrete column because the lateral reinforcement bar can apply confinement pressure on concrete core. Increase of strength and concrete ductility are the results of the confinement pressure which its value depends on the confinement pressure. In addition to lateral reinforcement bars, factors such as distribution method of longitudinal reinforcement bars and loading type affect the confinement.

Mander et al. [10] have provided an integrated tension-strain model for confined concrete with different sections under different loading conditions which is shown in Fig. 2. This compressive tension-strain diagram for confined concrete is achieved by the following equations.

$$f_c = \frac{f'_{cc} \cdot x}{r - 1 + x^r} \tag{1}$$

$$x = \frac{\varepsilon_c}{\varepsilon_{cc}} \tag{2}$$

$$r = \frac{E_c}{E_c - E_{sec}} \tag{3}$$

Where:

f'_{cc} :is the compressive strength (maximum tension) of the confined concrete,

ε_{cc} :is the maximum strain of confined concrete,

E_c :is the concrete tangant elactcity module,

E_{sec} :is the secant module of confined concrete in maximum tension.

Which is achieved by the following equation:

$$E_{sec} = \frac{f'_{cc}}{\varepsilon_{cc}} \tag{4}$$

Maximum strain of confined concrete is suggested by the following euqation:

$$\varepsilon_{cc} = \varepsilon_{co} \left[1 + 5 \left(\frac{f'_{cc}}{f'_{co}} - 1 \right) \right] \tag{5}$$

Where:

f'_{co} :is the unconfined concrete compressive tension,

ε_{co} :is the unconfined conccrete compressive strain.

The compressive strength of confined concrete (f'_{cc}) by the compressive strength of unconfined concrete (f'_{co}) and the effect of lateral confinement tension (f'_l) are determined which are presented by Mander et al. Confined concrete strength is determined by the following equation:

$$f'_{cc} = f'_{co} \left(-1.254 + 2.254 \sqrt{1 + \frac{7.94 f'_1}{f'_{co}}} - 2 \frac{f'_1}{f'_{co}} \right) \tag{6}$$

The effect of laternal confinement tension (f_l') is dependent on the volume ratio of laternal reinforcement bars, meshing and reinforcement form of longitudinal and transverse reinforcements and the area of internal effective concrete core. All equations are determined by Mander.

The tension-strain diagram for unconfined concrete is achieved by the Eq.1 and by replacing $(f_l' = 0)$ in Eq.6 and $(\varepsilon_{co} = 0.002)$ in Eq.5. Strength f_{co}' which is considered as concrete compressive strength is achieved by cylinder experiment. For unconfined concrete the 0.002 strain ε_{co} is acceptable. Considering the confinement by the lateral reinforcement bars, tension-strain diagram of partial confined concrete is determined.

Considering the concrete axial tension-strain diagram, we can say that this material shows linear behavior. Buy after that the concrete behavior is completely nonlinear. For introducing the concrete linear behavior, we need poisson coefficient and elesticity module. The preliminary elasticity module (E_{cc}) is achieved by Eq.7 which is determined from experiental relationships by ACI and also the confined concrete poisson coefficient is assumed as 0.2.

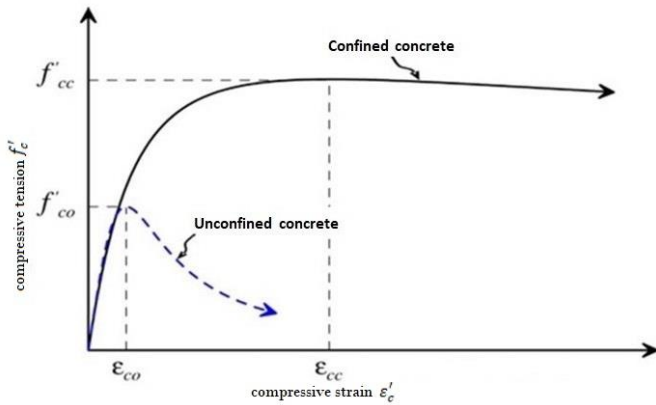$$E_{cc} = 5000\sqrt{f_{cc}'} \quad \text{MPa} \tag{7}$$

Fig 2. The diagram of tension-strain for confined and unconfined concrete which is presented by Mander [10].

2.2. Reinforcement

The elastic behavior of steel with elasticity module and Poisson coefficient values of 2×10^5 and 0.3, respectively is entered into the software. For defining the behavior, this behavior after the tension yield based on the plastic strain is entered into the software in table function format. Plastic strain is equal to the total strain and elastic strain. The relationship between total strains, plastic strain and elastic strain is as follows:

$$\varepsilon_{el} = \frac{\sigma}{E_s} \tag{8}$$

$$\varepsilon_{pl} = \varepsilon_t - \varepsilon_{el} \tag{9}$$

In the above relationships, E_s is the steel elastic module and ε_t, ε_{pl} and ε_{el} are elastic strain, plastic strain and total strain, respectively. And σ is the steel axial tension.

For modeling longitudinal reinforcements in concrete reinforcement or the composite members under flexural moment, an identical behavior under strain and compression is taken into consideration [8]. However, the buckling of longitudinal reinforcements occurs in inelastic big deformations in which the members are under compressive axial force. The buckling of longitudinal reinforcements has a meaningful effect on the strength and deformation of members. Considering the results, when the reinforcements experience buckling the loading capacity and deformation of reinforcements reduce which is shown in reinforcement bar experiments of Bayrak and Sheykh [11].

A simple model considering the inelastic bucking of longitudinal reinforcements under pressure is suggested which is shown in Fig. 3. The following assumptions are used for constructing a model; longitudinal reinforcements yield to the strength under pressure. When the axial strain reaches ε_{co} which is correspinding to maximum axial tension of unconfined concrete f_{co}' the reinforcement tension decreases. It is assumed that the

reinforcement bars buckle and lose their strength and this occurs by crushing the covered concrete when the concrete reaches its final strength. Reinforcement bar yield tension decreases to 20 percent of its yield strength and then maintains that strength.
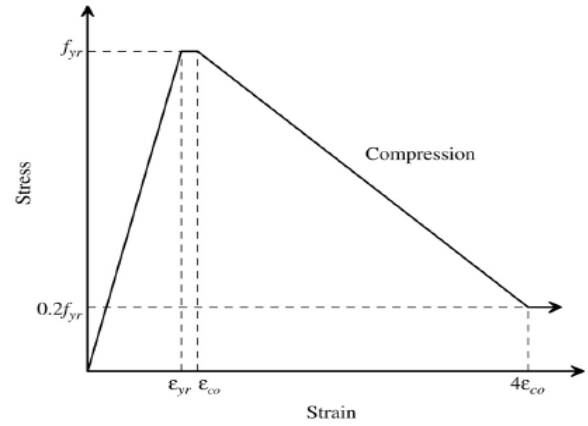

Fig 3. Strain-tension diagram for longitudinal reinforcement bars under pressure [8].

The reinforcement bars can be modeled by 3D elements or 2D elements (truss) buy there would be no meaningful different in their results. In case of using 3D elements in modeling the reinforcement bars, the dimensions and meshing in areas close to the reinforcement bars would be tiny. Therefore 1D elements (T3d2) would be used.

For modeling the relationship between reinforcement bars and concrete and also for modeling the performance of this material the adverb of "Embedded" would be used. This adverb would bury the reinforcement inside the concrete and calculates the reinforcement freedom degrees by interpolating the freedom degrees around the concrete.

2.3. Steel Section

The steel elastic behavior will be introduced by elasticity module and Poisson coefficient values of 2×10^5 and 0.3, respectively and also the identical strain-tension relationship which is achieved for the longitudinal reinforcements would be assumed for the structure steel section. As it is shown in Fig. 4, the local buckling of the elements, especially the steel member flange would likely occur after the concrete crush which is partially confined. Therefore, the decrease of tension after the axial strain reaches ε_{ccp} strain (strain corresponding to partially confined concrete compressive strength) is taken into consideration which shows the crush of partially confined concrete. When the axial strain reaches 4 times of the ε_{ccp} strain, the maximum strength corresspinding to 20 percent of yield strength would be taken into consideration [8].
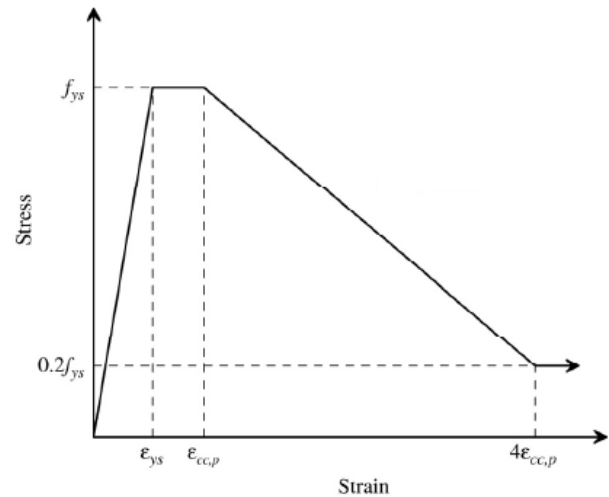

Fig 4. Tension-Strain diagram for steel section under pressure [8].

As concrete model, we use 8-node 3D elements (C3D8R) for modeling steel section. For modeling the contact between steel and concrete section and also the performance of this material an adverb called "surface to surface" is used. For using this adverb we need to define two levels which one of them is "master surface" and the other is the "slave surface" which concrete is considered as master surface near the steel section and the steel section is considered as the slave surface. The relationship between elements which is created by these two levels leads to a situation in which these two materials would have integrated performance and the slave surface displacement would ascribed to the master surface. When these two levels are in contact, the slave surface displacement would be recommended by a fraction coefficient which is 0.25 which is dependent on the master level. When these two levels are in contact, normal forces are transmitted through the master surface to the slave surface buy if these two levels act separately, there would be the displacement between two surfaces buy the normal forces would not transmitted through master surface to the slave surface, therefore two surface cannot act separately.

2.4. Boundary and Loading Conditions

For modeling loading sheets, discrete rigid 4-node 3D elements (R3D4) are used. The loading sheets are tied in the both ends of the column.

In this study the ends of both SRC columns are enclosed corresponding to three directions of X, Y, and Z and also bind in a circle corresponding to three direction. On the top of the columns and beam there is no possibility of displacement in Y and Z directions and only the applied load would be as 50 mm displacement along the x axis parallel with the beam.

3. Frame Modeling and Parametric Study

All sections are created in 3D space and as deformable and the analysis is general and static. The connection of frame members would be defined as abovementioned. And the nonlinearity of masonry and geometry would be taken into consideration in modeling.

In this study three frame sample would be used and in all frames we use confined concrete steel composite with 160×160 dimension, 1000 mm height and a beam with 1000 mm length (Fig. 5). In frame number 1 the SRC composite beam with specifications according to table 1 would be used. The frame number 2 with steel section beam is modeled and its dimensions and masonry specifications are as table 2 and finally based on table 3 the reinforced concrete beam is used for modeling the frame number 3.

In this research we study the effect of increasing concrete compressive strength and steel yield tension on the behavior of frame under monotonic loading. For each frame sample, the concrete compressive strength (f_c) is 30 and 70 MPa, steel section yield tension (f_{ys}) is 360 and 690 MPa and reinforcement yield tension (f_{yr}) is 400 MPa. The distance of stirrup s (S) in all columns is 125 mm and in all beams is 100 mm. four longitudinal reinforcements with 4 mm diameters and 6 mm transverse reinforcements are used in sections.
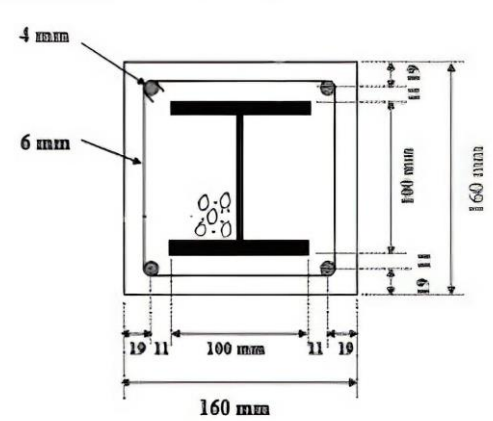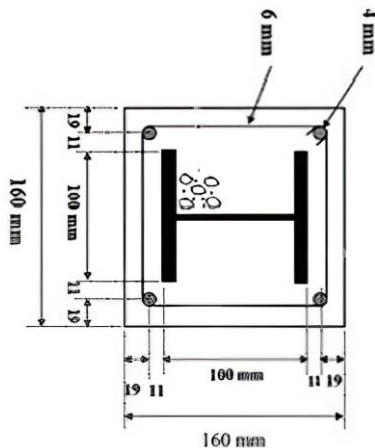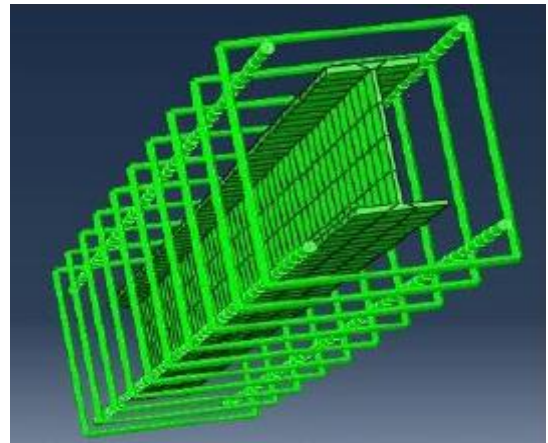

Column
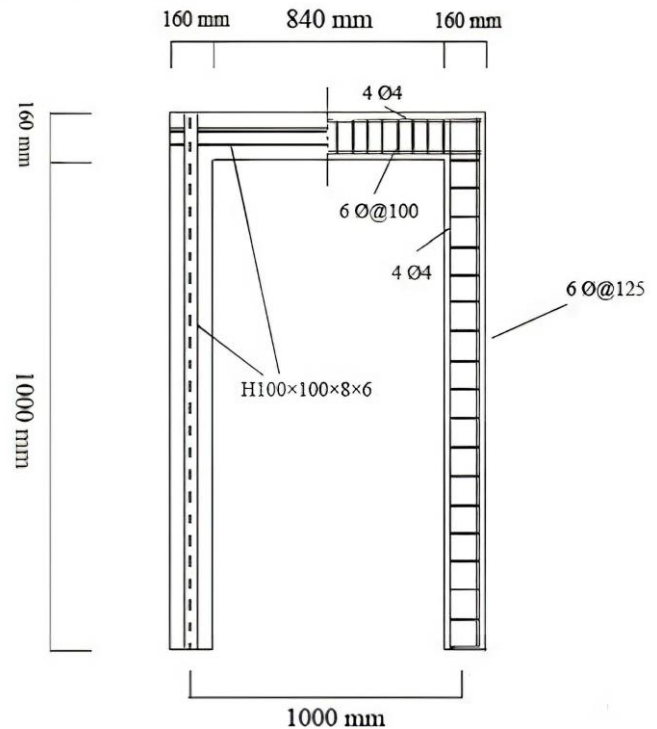
Frame

Fig 5. Specifications of beam, columns, and frame sections.

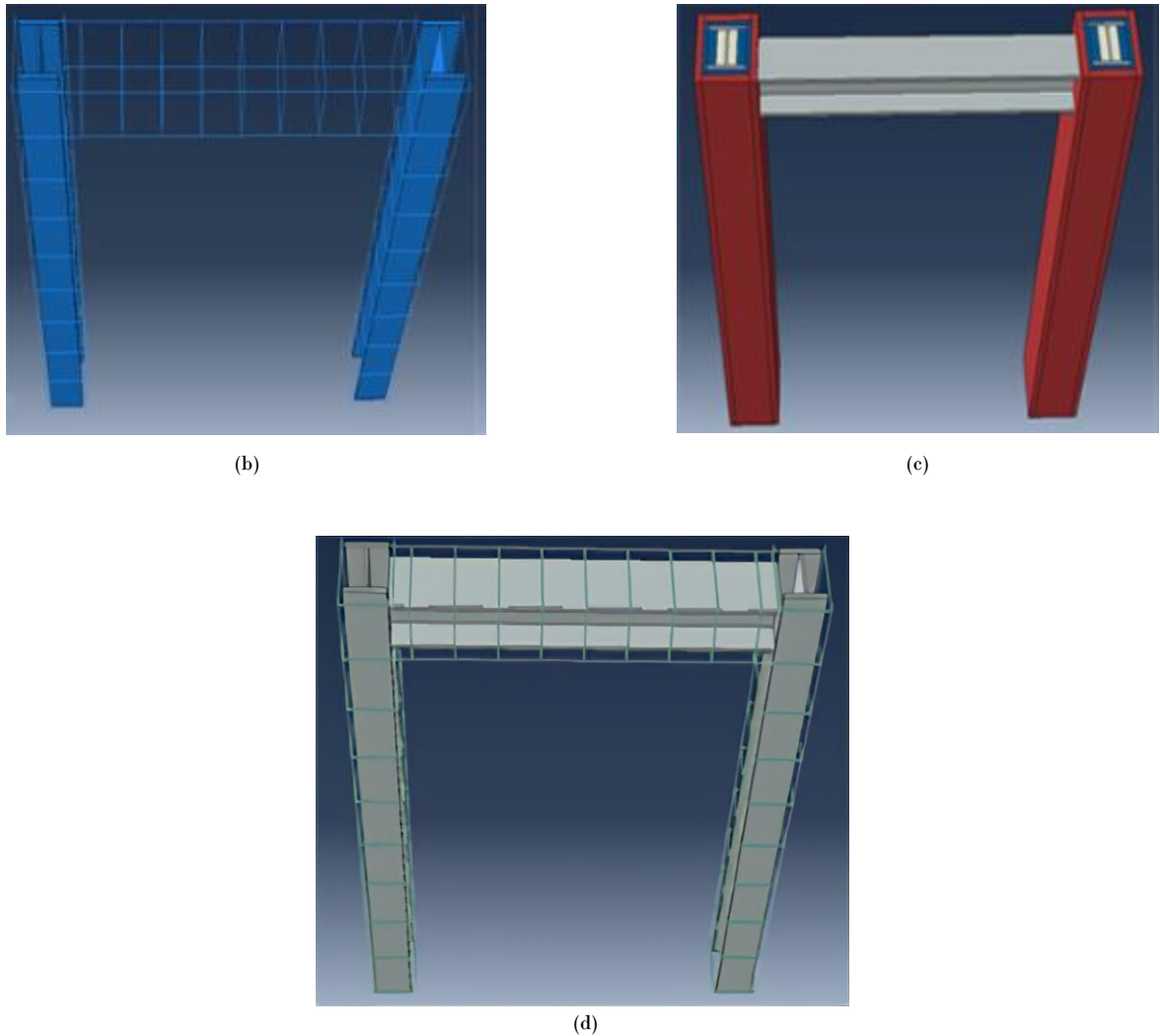Beam

(a)

(b)

(c)

(d)

Fig 6. Modeled frames. a) Finite element model of steel section with reinforcements, b) Frame with reinforced concrete beam, c) Frame with steel beam, d) Frame with concrete-confined steel composit beam.

Table 1. Specifications of dimensions and masonry of frame with SRC beam.

Sample		Height (mm)	Steel Profile (mm)	F$_c$ (MPa)	F$_{ys}$ (MPa)	F$_{yr}$ (MPa)	Longitudinal reinforcement		Transverce reinforcement	
							No	Ø	Ø	S
Frame 1	Column	1000	H100×100×8×6	30	240	400	4	4	6	125
	Beam	1000	H100×100×8×6	30	240	400	4	4	6	100
Frame 2	Column	1000	H100×100×8×6	70	240	400	4	4	6	125
	Beam	1000	H100×100×8×6	70	240	400	4	4	6	100
Frame 3	Column	1000	H100×100×8×6	30	690	400	4	4	6	125
	Beam	1000	H100×100×8×6	30	690	400	4	4	6	100
Frame 4	Column	1000	H100×100×8×6	70	690	400	4	4	6	125
	Beam	1000	H100×100×8×6	70	690	400	4	4	6	100

Table 2. Specifications of dimensions and masonry of frame with steel beam.

Sample		Height (mm)	Steel Profile (mm)	F$_c$ (MPa)	F$_{ys}$ (MPa)	F$_{yr}$ (MPa)	Longitudinal reinforcement		Transverce reinforcement	
							No	Ø	Ø	S
Frame 9	Column	1000	H100×100×8×6	30	240	400	4	4	6	125
	Beam	1000	H100×100×8×6	30	240	400	-	-	-	-
Frame 10	Column	1000	H100×100×8×6	70	240	400	4	4	6	125
	Beam	1000	H100×100×8×6	70	240	400	-	-	-	-
Frame 11	Column	1000	H100×100×8×6	30	690	400	4	4	6	125
	Beam	1000	H100×100×8×6	30	690	400	-	-	-	-
Frame 12	Column	1000	H100×100×8×6	70	690	400	4	4	6	125
	Beam	1000	H100×100×8×6	70	690	400	-	-	-	-

**Table 3.** Specifications of dimensions and masonry of frame with reinforcement concrete beam.

Sample		Height (mm)	Steel Profile (mm)	F_c (MPa)	F_{ys} (MPa)	F_{yr} (MPa)	Longitudinal reinforcement		Transverce reinforcement	
							No	∅	∅	S
Frame 5	Column	1000	H100×100×8×6	30	240	400	4	4	6	125
	Beam	1000	H100×100×8×6	30	240	400	4	4	6	100
Frame 6	Column	1000	H100×100×8×6	70	240	400	4	4	6	125
	Beam	1000	H100×100×8×6	70	240	400	4	4	6	100
Frame 7	Column	1000	H100×100×8×6	30	690	400	4	4	6	125
	Beam	1000	H100×100×8×6	30	690	400	4	4	6	100
Frame 8	Column	1000	H100×100×8×6	70	690	400	4	4	6	125
	Beam	1000	H100×100×8×6	70	690	400	4	4	6	100

4. Results

Considering the table 4, by increase of concrete compressive strength and steel section yield tension, the frame strength is also increased which the effect of increasing concrete compressive strength on the increase of frame strength is more than the increase of steel sectio yield tension. Also, the increase of concrete compressive strength fore concrete with steel section yield tension of 240 MPa has more pronunced effect on the increase of frame strength with steel section yield tension of 690 MPa.
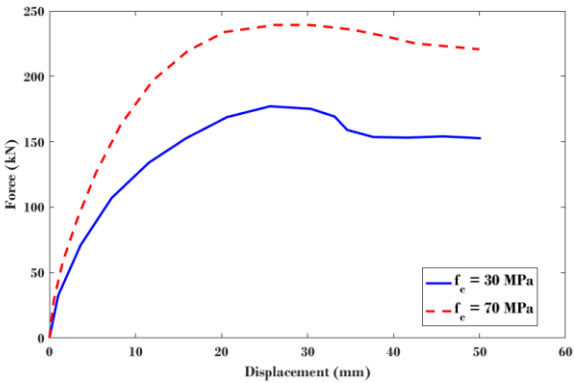
Table 4. Results of FEA of frame with SRC beam.

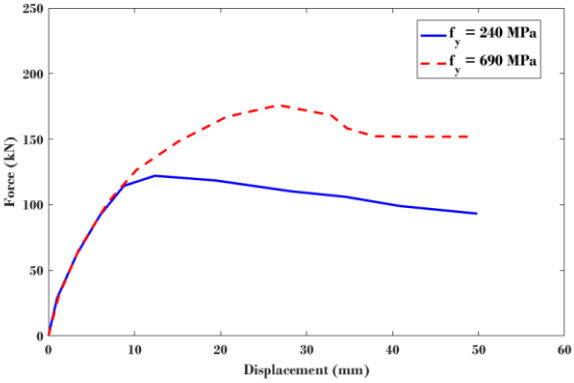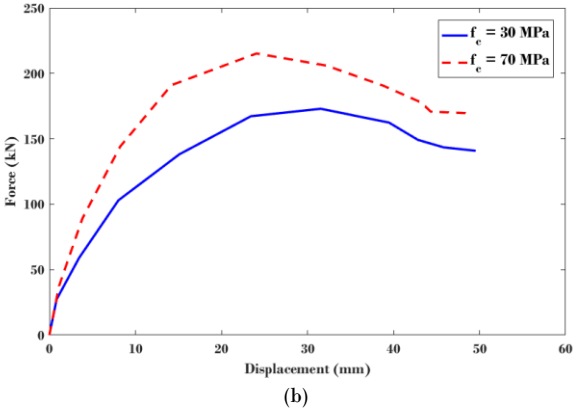| Sample	P_y(kN)	Δ_y(mm)	Δ_u(mm)	μ
Frame 1	121.78	7	36.2	5.17
Frame 2	188.5	7.25	33.6	4.63
Frame 3	176.13	12.2	48.9	4
Frame 4	239.2	11.2	49.6	4.43

(a)

(a)
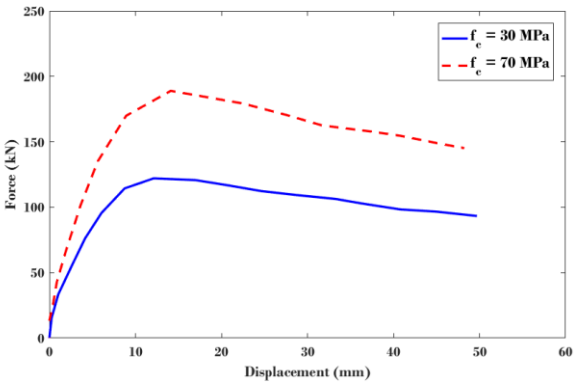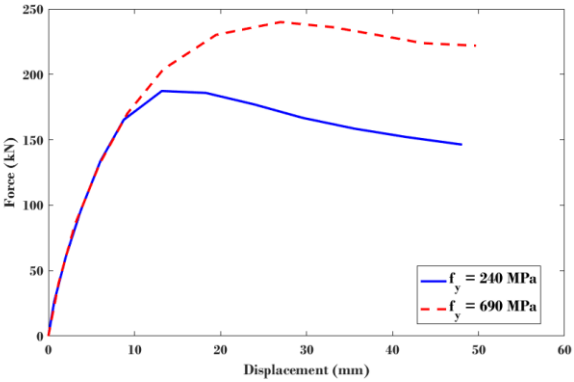
(b)

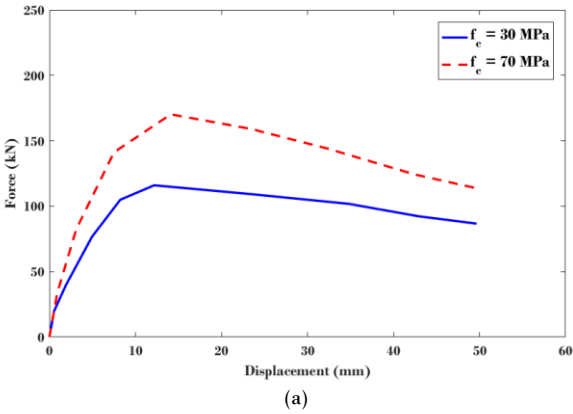**Fig 7.** The effect of increasing compressive strength on the frame with SRC beam, a) steel yield tension 240 MPa, b) steel yield tension 690 MPa.
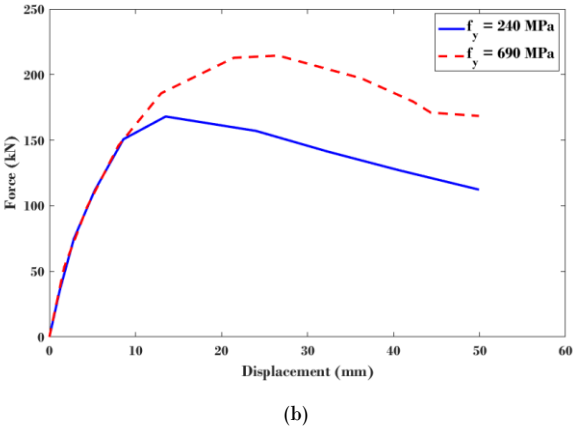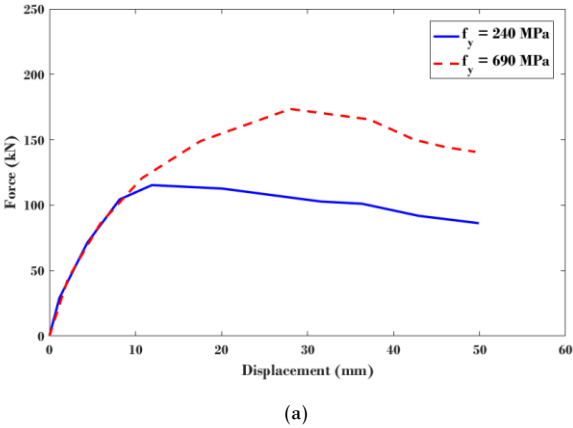

(b)

Fig 8. The effect of increasing steel section yield tension on frame wth SRC beam, a) compressive strength 30 MPa, b) compressive strength 70 MPa.

Consiering the table 5 by increase of concrete compressive strength and steel section yield tension, the frame strength also increases and also the parameter of steel section yield tension has more pronounced effect on increase of frame strength with steel beam so the increase of yield tension for compressive strength of 30 MPa has more prononced effect than the frame with compressive strength of 70 MPa.

Table 5. Results of FEA of frame with steel beam.

Sample	P_y(kN)	Δ_y(mm)	Δ_u(mm)	μ
Frame 5	116.4	7	37.82	5.4
Frame 6	170	7.25	31.8	3.98
Frame 7	176.13	12.2	42	3.36
Frame 8	216.06	11.2	41.3	3.59

(a)

Consiering the table 6 by increase of concrete compressive strength and steel section yield tension, the frame strength also increases and also the two parameters of steel section yield tension and concrete compressive strengt have almost dentical effect on increase of frame strength with reinforcement concrete beam and increase of these two parameters on the frame with compressive strength of 30 MPa and steel yield tension has more prononced effect.

Table 6. Result of FEA of frame with reinforced concrete beam.

Sample	P_y(kN)	Δ_y(mm)	Δ_u(mm)	μ
Frame 9	121.36	6.7	32.6	4.86
Frame 10	178.32	7.3	28.8	3.94
Frame 11	173.65	12.1	41.5	3.43
Frame 12	219.79	10	37.3	3.73

(b)

Fig 9. The effect of compressive strength on the frame with steel beam, a) steel yield tension 240 MPa, b) steel yield tension 690 MPa.
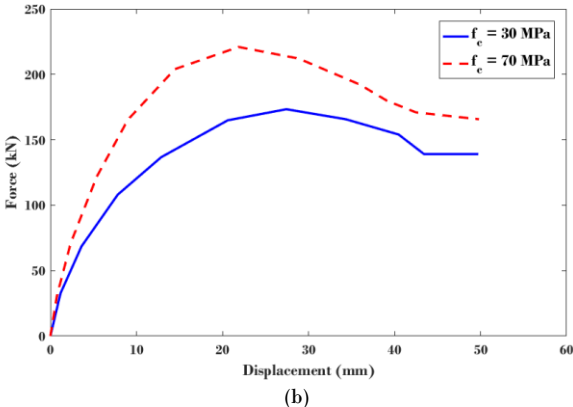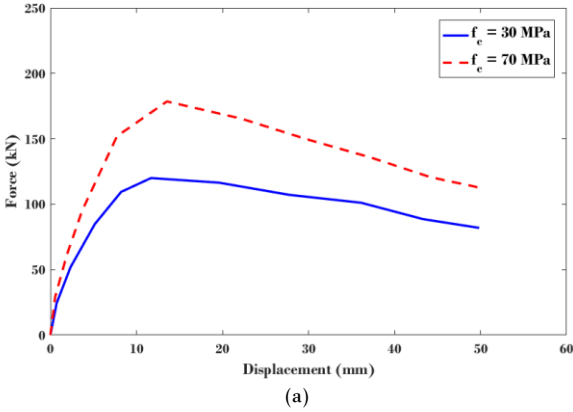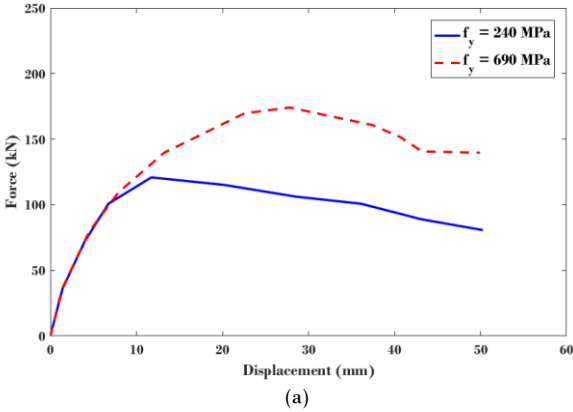

(a)

(b)

Fig 11. The effect of increase of compressive strength on the frame with reinforcement concrete beam, a) steel yield tension 240 MPa, b) steel yield tension 690 MPa.
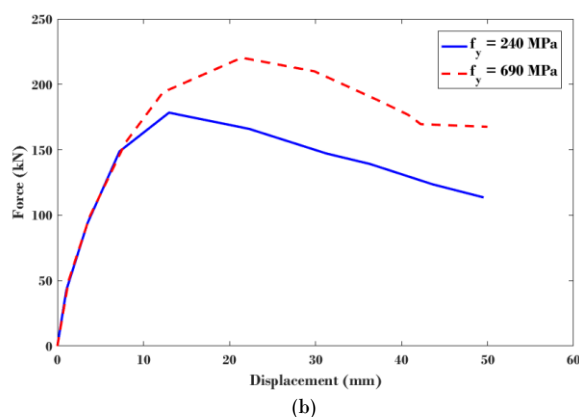

(a)

(b)

Fig 10. The effect of increasing steel section yield tension on frame wth steel beam, a) compressive strength 30 MPa, b) compressive strength 70 MPa.

(a)

(b)

Fig 12. The effect of increasing steel section yield tension on frame wth reinforced concrete beam, a) compressive strength 30 MPa, b) compressive strength 70 MPa.

5. Conclusions

In frame with SRC column and SRC beam the increase of concrete compressive strength has more effect on the increase of frame strength. By 70 MPa increase of concrete compressive strength for frame with compressive strength of 30 MPa and yield tension of 240 MPa, the frame strength would increase by 54.8%.

In frame with SRC column and steel section beam the increase of steel section yield tension has more effect on the increase of frame strength. By 690 MPa increase in steel yield tension for frame with 30 MPa compressive strength and 240 MPa yield tension the frame strength would increase by 46%.

In frame with SRC column and reinforced concrete beam, increase of concrete compressive strength and increase of steel section yield tension have also identical effect on increase of frame strength. The increase of concrete compressive strength by 70 MPa for frame with 30 MPa compressive strength and 240 yield tension, the frame strength would increase by 46.93% and by increase of steel yield tension from 240 MPa to 690 MPa, the frame strength would increase by 43.1%.

All three types of frames with compressive strength of 30 MPa have almost identical yield strength, while fore compressive strength of 70 Mpa, the frame with SRC beam is stronger than two other frames.

Conflict of interest

There is not conflict of interest.

References

[1]. Kong, J., Zou, Y., Wan, Z. W., & Li, C. (2013). Nonlinear numerical analysis of SRC Frame Joint. *Applied Mechanics and Materials*, (405–408), 1191–1195.
https://doi.org/10.4028/www.scientific.net/amm.405-408.1191
[2]. Kong, J., Zou, Y., Li, C., & Wan, Z. W. (2013). Nonlinear Numerical Analysis of SRC Frame End Joint. *Advanced Materials Research*, 753–755, 1151–1155.
https://doi.org/10.4028/www.scientific.net/amr.753-755.1151
[3]. Li, K. W., Li, Z. Y., Wan, X., & Liu, F. (2015). Non-Linear Numerical Simulation on Hysteretic Behavior of SRC Columns. *Applied Mechanics and Materials*, 723, 382–386.
https://doi.org/10.4028/www.scientific.net/amm.723.382
[4]. Alavi, R., and Izadinia, M. (2012). A review of statute design and numeral modeling of concrete-confined steel composite columns. *The first national conference of durable construction, Mashhad.*
[5]. Kheyroldin, A., Naderpour, H., and Ahamdi, M. (2012). Study of concrete confinement effect under steel wall in concrete composite circle columns. *The second national conference of crisis management, Tehran.*
[6]. Beiranvand, P., Abdollahifar, M., Moradpour, A., Sadeghi Golmakani, S. (2019). Investigation of load capacity of steel concrete composite columns SRC reinforced by IPE. *Civil and Environmental Engineering Reports*, 29(2), 101-116.
https://doi.org/10.2478/ceer-2019-0019

[7]. Mirza, S. A. (1989). Parametric study of composite column strength variability. *Journal of Constructional Steel Research*, 14(2), 121–137. https://doi.org/10.1016/0143-974x(89)90019-9
[8]. Chen, C. C., and Lin, N. J. (2006). Analytical model for predicting axial capacity and behavior of concrete encased steel composite stub columns. *Journal of Constructional Steel Research*, 62(5), 423-424.
https://doi.org/10.1016/j.jcsr.2005.04.021
[9]. Mirza, S. A., and Skrabek, B. W. (1992). Statistical analysis of slender composite beam-column strength. *Journal of Structural Engineering*, 118(5), 1312.
https://doi.org/10.1061/(ASCE)0733-9445(1992)118:5(1312)
[10]. Mander, J. B., Priestley, M. J. N., and Park, R. (1988). Theoretical stress–strain model for confined concrete. *Journal of Structural Engineering*, 114(8), 1804–1826.
https://doi.org/10.1061/(ASCE)0733-9445(1988)114:8(1804)
[11]. Bayrak, O., and Sheikh, S. A. (2001). Plastic hinge analysis. *Journal of Structural Engineering*, 127(9), 1092.
https://doi.org/10.1061/(ASCE)0733-9445(2001)127:9(1092)